

# A novel quantum dot pillared layered transition metal sulfide: CdS–MoS<sub>2</sub> semiconductor–metal nanohybrid

Jin-Kyu Lee,<sup>\*a</sup> Woo Lee,<sup>a</sup> Tae-Jong Yoon,<sup>a</sup> Gyeong-Su Park<sup>b</sup> and Jin-Ho Choy<sup>\*c</sup>

<sup>a</sup>School of Chemistry and Molecular Engineering, Seoul National University, Seoul 151-747, Korea. E-mail: jinklee@snu.ac.kr

<sup>b</sup>Samsung Advanced Institute of Technology, Post Office Box 111, Suwon 440-660, Korea

<sup>c</sup>National Nanohybrid Materials Laboratory, School of Chemistry, Seoul National University, Seoul 151-747, Korea. E-mail: jhchoy@plaza.snu.ac.kr

Received 5th September 2001, Accepted 22nd November 2001

First published as an Advance Article on the web 28th January 2002

A novel metal–semiconductor and/or heterodimensional nanohybrid material (CdS–MoS<sub>2</sub>) is synthesized by hybridizing catalytically important materials (*i.e.*, zero-dimensional CdS quantum dots and two-dimensional, unilamellar MoS<sub>2</sub> sheets). According to our high-resolution transmission electron microscopic (HRTEM) analyses on the present nanohybrid, *ca.* 6.5 nm CdS quantum dots are successfully immobilized in the interlayer space of MoS<sub>2</sub> sheets. The microscopic internal structure of the CdS–MoS<sub>2</sub> nanohybrid is mainly characterized as a ‘house of cards’ structure. Such a microscopic evolution is further demonstrated by BET specific surface area analyses. The BET surface area ( $\sim 84 \text{ m}^2 \text{ g}^{-1}$ ) of the present nanohybrid sample is nearly two orders of magnitude larger than that of the pristine material (2H–MoS<sub>2</sub>), suggesting that the CdS quantum dots are rather loosely packed in the interlayer space of MoS<sub>2</sub> platelets to create many voids. We suggest, from the observed microscopic evolution and the increased BET surface area, that the present nanohybrid material can be successfully applied as a high performance catalyst in hydrodesulfurization (HDS) and/or visible light harvesting photocatalyst.

## Introduction

The synthesis and manipulation of materials on the nanometer and subnanometer scale are currently intense areas of research for designing and fabricating new functional materials with optical, conductive/superconductive, catalytic and biological applications. Therefore, we developed hybridization techniques by combining physicochemically dissimilar materials into well organized heterostructural architectures like inorganic–inorganic,<sup>1</sup> organic–inorganic,<sup>2</sup> and bio-inorganic<sup>3</sup> hybrid structures. These have been utilized to generate advanced nanohybrid materials since they allow us not only to exploit two or more desirable properties but also to provide additional stability for otherwise highly labile structures. Previously, organic molecules or conducting polymer composites of MoS<sub>2</sub> were synthesized by aqueous exfoliation of lithiated MoS<sub>2</sub> and by subsequent restacking of a unilamellar suspension around the guest molecules.<sup>4–6</sup> However, relatively little is known about nanocluster pillared hybrid materials, although an example has recently been demonstrated of the intercalation of the molecular clusters (Co<sub>6</sub>Q<sub>8</sub>(PR<sub>3</sub>)<sub>6</sub>; Q = S, Se, and Te and R = alkyl) into MoS<sub>2</sub> by Kanatzidis *et al.*<sup>7</sup> Herein we report the synthesis and microscopic characterization of the novel quantum dot pillared transition metal dichalcogenide (CdS–MoS<sub>2</sub>). In view of the application of a hybridization technique, the present material can be regarded as a metal–semiconductor and/or heterodimensional nanohybrid material since the exfoliated two-dimensional MoS<sub>2</sub> sheets have proven to be metallic conductors,<sup>8,9</sup> whilst the zero-dimensional CdS quantum dot is a semiconductor. Moreover, the precursor materials used in the present study could have attracted particular interest among materials scientists because of their technological importance for catalytic applications (*i.e.*, a hydrodesulfurization (HDS) catalyst and a visible light harvesting photocatalyst for MoS<sub>2</sub> and CdS nanoparticles, respectively).<sup>10</sup>

## Experimental

A reverse micellar system consisting of sodium bis(2-ethylhexyl)sulfosuccinate (AOT, 100 mM), water and n-heptane was used. CdS nanocrystallites were prepared by the rapid addition of 10 ml heptane solution of S(TMS)<sub>2</sub> ( $8.0 \times 10^{-4} \text{ M}$ ) to an AOT–heptane micellar solution {300 ml, W<sub>o</sub> (= [H<sub>2</sub>O]/[AOT]) = 5.4} containing Cd(ClO<sub>4</sub>)<sub>2</sub>·6H<sub>2</sub>O ( $6.0 \times 10^{-3} \text{ M}$ ) with vigorous stirring for 2 h at room temperature. Surface passivation of CdS nanocrystals with thiophenolate was achieved by adding thiophenolate ( $8.0 \times 10^{-4} \text{ M}$ , 0.8 ml) to the resulting mixture. Following the addition of pyridine for elimination of the reverse micelles, the thiophenolate-capped CdS (which hereafter will be denoted as CdS(TP)<sub>n</sub>), was collected by centrifugation. The transparent and intense yellow solution of CdS(TP)<sub>n</sub> was obtained by redispersing the resulting precipitate in neat methyl isobutyl ketone (MIBK).

Complete delamination of MoS<sub>2</sub> was achieved by exfoliating lithiated MoS<sub>2</sub> in deionized water *via* a redox reaction as reported;<sup>5</sup> MoS<sub>2</sub> powder was stirred in a 1.6 M hexane solution of n-butyllithium for 48 h under nitrogen at room temperature. The solid product was collected by centrifuging the reaction mixture and then washed with hexane. Then, the resulting LiMoS<sub>2</sub> was immersed in deionized water and stirred for several hours to give a unilamellar suspension of MoS<sub>2</sub>. The exfoliated suspension was centrifuged and washed five times with copious amounts of water to ensure the complete removal of LiOH (the final pH should reach *ca.* 7), then resuspended again in deionized water.

Cross-sectional TEM specimens of the [CdS(TP)<sub>n</sub>]<sub>0.086</sub>–MoS<sub>2</sub> nanohybrid materials were prepared as described below. The [CdS(TP)<sub>n</sub>]<sub>0.086</sub>–MoS<sub>2</sub> nanohybrids were embedded in acrylic resin (methyl methacrylate : n-butyl methacrylate = 4 : 6, benzoyl peroxide 1.5%) in a polyethylene capsule. The embedded [CdS(TP)<sub>n</sub>]<sub>0.086</sub>–MoS<sub>2</sub> nanohybrids were ultramicrotomed using a diamond knife to produce thin specimens

for high-resolution transmission electron microscopy (HRTEM) study. The slicing speed and thickness were set at  $1 \text{ mm s}^{-1}$  and  $60 \text{ nm}$ , respectively. The thin sections were then located onto a carbon coated microgrid and immersed in chloroform to remove the acrylic resin. HRTEM study was carried out with a Hitachi H-9000NA TEM at an accelerating voltage of  $300 \text{ kV}$ .

## Results and discussion

### Characterization of exfoliated $\text{MoS}_2$

Successful delamination of the pristine  $2\text{H-MoS}_2$  into single molecular sheets was confirmed by HRTEM on a freshly exfoliated sample. A representative cross-sectional HRTEM image of the exfoliated sample is presented in Fig. 1. Unlike the image of highly ordered and rigid stacks of  $\text{MoS}_2$  planes along the  $c$ -direction which is expected in the pristine  $2\text{H-MoS}_2$ , the micrograph of the exfoliated sample exhibits severely distorted or highly flexible single sheets of  $\text{MoS}_2$  and layer packets that are originated from partial restacking of elementary chalcogenide sheets.<sup>11</sup> A magnified view of some part of the present micrograph is also presented as an inset figure. The estimated  $c$ -axis dimension (*ca.*  $6.2 \text{ \AA}$ ) of unilamellar  $\text{MoS}_2$  sheets is consistent with the X-ray crystallographically determined thickness of single  $\text{MoS}_2$  layers of the pristine material, manifesting again complete exfoliation of  $\text{MoS}_2$ .

Fig. 2(a) and (b) show selected area electron diffraction (SAED) patterns of the pristine ( $2\text{H-MoS}_2$ ) and exfoliated–restacked  $\text{MoS}_2$ , respectively. The samples for the examination of electron diffraction (ED) patterns were prepared by depositing the aqueous suspension of the pristine  $\text{MoS}_2$  or

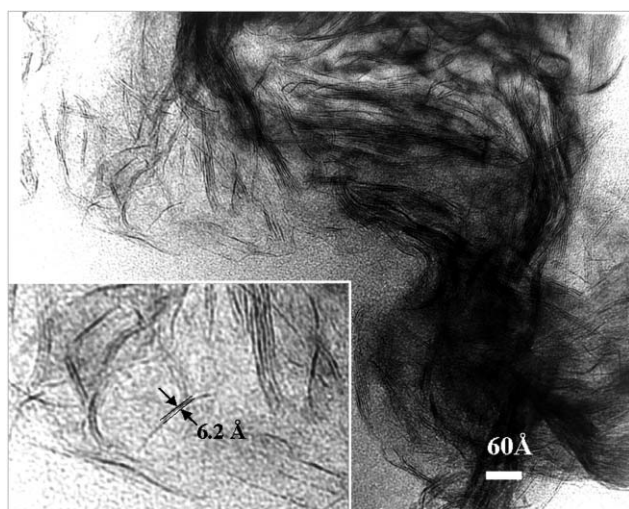


**Fig. 1** Cross-sectional HRTEM image of restacked  $\text{MoS}_2$ . The inset shows that exfoliation reaction leads to complete delamination of bulk  $\text{MoS}_2$  into single molecular sheets.

its exfoliate on carbon-coated copper grids and then evaporating the solvent. As expected from the platelike morphology of layered materials, the present diffraction patterns contain only  $[hk0]$  information owing to the preferred sample orientations, which cause the  $ab$ -plane to be perpendicular to the electron beam. It becomes clear from Fig. 2 that the exfoliation reaction leads to structural transformation. The electron diffraction patterns of the exfoliated–restacked sample can be indexed with  $\sqrt{3}a \times a$ -type superstructure ( $a =$  lattice parameter of  $2\text{H-MoS}_2$ ) of trigonal symmetry, consistent with the result of Heising *et al.*<sup>12</sup> Such a structural transformation is related to the change of local symmetry around the molybdenum atom from trigonal prismatic symmetry ( $D_{3h}$ ) in the pristine  $2\text{H-MoS}_2$  to octahedral symmetry ( $O_h$ ) in the exfoliated–restacked  $\text{MoS}_2$ . In the  $\text{Mo(IV)}$  system with  $d^2$ -electron configuration, the trigonal prismatic symmetry develops a semiconductive band gap between the filled  $d_{z^2}$  and empty  $d_{x^2-y^2,xy}$  bands, whereas the octahedral one produces a metallic band structure due to a partially filled single band that is formed from the degenerated  $d_{xy,yz,xz}$  orbitals.<sup>4–6</sup> In fact, the metallic conductivity of restacked  $\text{MoS}_2$  has been demonstrated by temperature dependent magnetic susceptibility or thermoelectric power measurement.<sup>8</sup>

### Nanohybrid synthesis

The  $[\text{CdS}(\text{TP})_n]_{0.086}\text{-MoS}_2$  nanohybrid material has been realized by adding a yellow-colored MIBK solution of thiophenol ( $\text{C}_6\text{H}_5\text{SH}$ ) capped CdS nanoparticles to the black aqueous suspension of exfoliated  $\text{MoS}_2$ . Reaction occurs at the interface of water and organic solvent (MIBK), where black flocculi of  $\text{MoS}_2$  containing CdS quantum dots are formed. With 30 min of stirring, the black-colored aqueous layer of single sheet  $\text{MoS}_2$  completely clears and the color of the organic layer turns pale yellow, suggesting that CdS nanoparticles migrate from the organic solution to the organic–aqueous interface and form a hybrid composite with exfoliated  $\text{MoS}_2$ . One can completely decolorize the organic layer by introducing additional aqueous  $\text{MoS}_2$  suspension into the reaction vessel. The products were isolated by vacuum filtration, thoroughly washed with the appropriate solvent to remove any extraneous clusters, and finally dried under vacuum overnight.

In contrast to the long reaction time ( $>2$  days) for the synthesis of neutral species intercalated  $\text{MoS}_2$ ,<sup>4–6</sup> where a decrease in negative charge per Mo atom by gradual oxidation of  $\text{MoS}_2$  sheets over time might proceed prior to encapsulation of neutral guests, the rapid formation ( $<30$  min) of the present quantum dot pillar at the interface of water and organic solvent (MIBK) can be attributed to an ionic interaction between two oppositely charged inorganic species. Previously, Heising *et al.* reported that the negative charge on the  $\text{MoS}_2$  layers is between  $0.1$  and  $0.4 e^-$  per Mo atom, based on their experimental findings on the number of cationic clusters,  $\text{Al}_3\text{O}_4(\text{OH})_{24}\text{-(H}_2\text{O)}_{12}^{7+}$ , loaded on  $\text{MoS}_2$ .<sup>13</sup> More recently, the same group

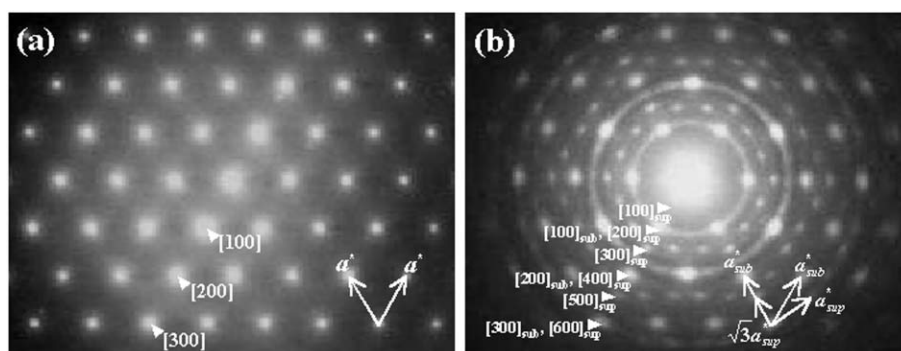


**Fig. 2** Selected area electron diffraction (SAED) patterns of (a) the pristine  $2\text{H-MoS}_2$  and (b) exfoliated–restacked  $\text{MoS}_2$ .

**Table 1** Observed and calculated weight percentage of each element in the pristine MoS<sub>2</sub> and (CdS)<sub>0.086</sub>MoS<sub>2</sub> nanohybrid

Element	Pristine MoS <sub>2</sub>		(CdS) <sub>0.086</sub> MoS <sub>2</sub>	
	atom% (obs.) <sup>a</sup>	atom% (calc.) <sup>b</sup>	atom% (obs.) <sup>a</sup>	atom% (calc.) <sup>c</sup>
Cd	—	—	2.655	2.711
Mo	31.994	33.333	30.849	31.526
S	68.006	66.667	66.496	65.763

<sup>a</sup>Average values obtained from seven EPMA measurements for each sample. <sup>b</sup>The theoretical values were calculated with the nominal composition of MoS<sub>2</sub> for the pristine compound. <sup>c</sup>The theoretical values were calculated with the composition of (CdS)<sub>0.086</sub>MoS<sub>2</sub>, which was based on the observed atomic ratio of the metals (Cd : Mo).

reported that the range of negative charge on single sheet MoS<sub>2</sub> is 0.1–0.25 e<sup>-</sup> per Mo atom, which was determined by chemical analyses on alkali metal cations encapsulated in MoS<sub>2</sub> layers.<sup>9</sup> Accordingly, since single sheets of MoS<sub>2</sub> in aqueous suspension can be regarded as solvated macroanions whose surfaces are negatively charged, it is believed that the surfaces of CdS(TP)<sub>n</sub> crystallites in MIBK are positively charged. In fact, from our surface charge measurements using electrophoresis apparatus, it was observed that the present CdS(TP)<sub>n</sub> dots exhibit a net drift toward the cathode, manifesting positively charged surfaces. The origin of such positive surface charge could be attributed to insufficient cap density on the surface of CdS nanocrystallites. Since smaller particles have higher surface curvature and less continuous surfaces emerge,<sup>14,15</sup> positive surface charges in smaller particles could not be effectively screened due to steric crowding of capping molecules. This speculation might be supported by our control experiments with smaller-sized CdS(TP)<sub>n</sub> (ca. 1 nm); as the size of CdS(TP)<sub>n</sub> decreases, the time required to reach full equilibrium for the formation of CdS(TP)<sub>n</sub> pillar decreases.

### Electron microscopic analysis on (CdS(TP)<sub>n</sub>)<sub>0.086</sub>-MoS<sub>2</sub> nanohybrid

The morphology of the present nanohybrid (CdS(TP)<sub>n</sub>)<sub>0.086</sub>-MoS<sub>2</sub> was investigated by a field emission-scanning electron

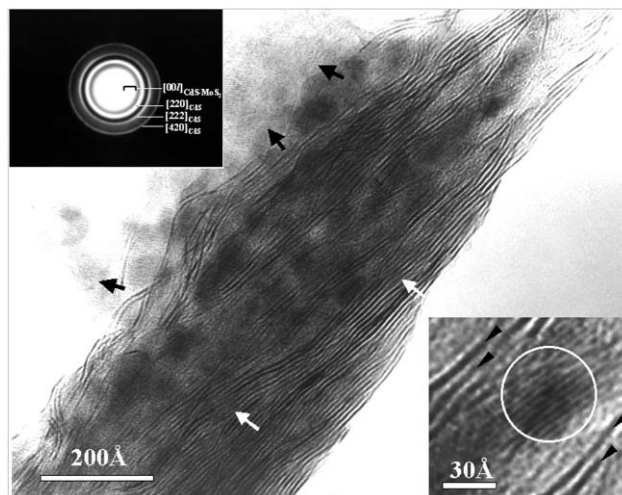


**Fig. 4** A cross-sectional HRTEM image of (CdS(TP)<sub>n</sub>)<sub>0.086</sub>MoS<sub>2</sub> nanohybrid that was obtained from the edge part of a cross-sectioned specimen. The upper-left insert shows a selected area electron diffraction (SAED) pattern of the sample. The insert at the down-right corner shows a magnified HRTEM image, showing a pillared CdS quantum dot (white circle) at the interlamellar space of MoS<sub>2</sub> sheets (black triangles).

microscope (FE-SEM; Hitachi S-4300) in conjunction with EDAX for quantitative analyses. Fig. 3 presents representative SEM images from the quantum dot pillared MoS<sub>2</sub> under different magnifications. When the as-prepared samples are dispersed on a planar substrate, aggregates of quantum dot pillared MoS<sub>2</sub> sheets exhibit coralloid morphology rather than well-oriented platelets in contrast to our expectations [Fig. 3(a)]. Such a morphological evolution might have originated from external stress arising in the course of product isolation (*i.e.*, vacuum filtration and intensive washing), and is reminiscent of the highly disordered internal structure of (CdS(TP)<sub>n</sub>)<sub>0.086</sub>MoS<sub>2</sub> nanohybrids. From close examination of the present morphology and EDAX analyses<sup>16</sup> in the course of the microscopic investigation, it is evident that the sample consisted of highly flexible unilamellar sheets of MoS<sub>2</sub> and spherical CdS(TP)<sub>n</sub> nanocrystallites, where quantum dots are believed to be wrapped inside wrinkled MoS<sub>2</sub> sheets forming an uneven and embossed surface morphology [inset of Fig. 3(b)].

The presence of CdS(TP)<sub>n</sub> nanoclusters in MoS<sub>2</sub> sheets was further demonstrated by HRTEM (Hitachi H-9000NA). Two distinct structural features could be discerned from the micrographs. In the edge region of the cross-sectioned specimen, microscopic evolution is mainly characterized by partially delaminated, completely pillared and unpillared structures of well-oriented MoS<sub>2</sub> sheets, and CdS(TP)<sub>n</sub> rich domains [Fig. 4]. Upon closer inspection of the present micrographs, it is clear that there is partial extrusion of CdS(TP)<sub>n</sub> nanocrystallites from the interlamellar space of restacked MoS<sub>2</sub> sheets, which

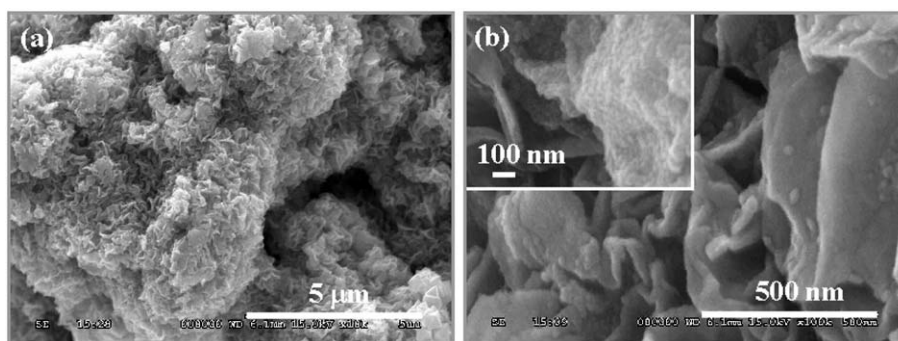


**Fig. 3** SEM micrographs of the (CdS(TP)<sub>n</sub>)<sub>0.086</sub>MoS<sub>2</sub> nanohybrid under (a) low magnification and (b) high magnification. Inset in (b) shows that the sample consists of spherical CdS nanocrystallites, which are believed to be wrapped inside wrinkled MoS<sub>2</sub> sheets.

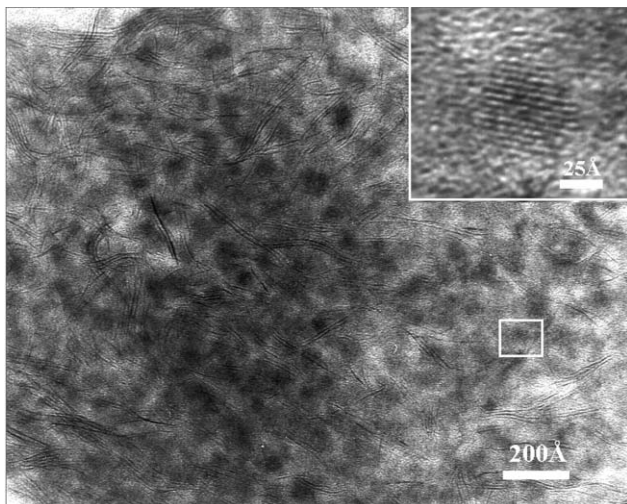


**Fig. 5** A cross-sectional HRTEM image of the inner region of a thin-sectioned  $(\text{CdS}(\text{TP})_n)_{0.086}\text{MoS}_2$  nanohybrid. One of the dark dots (white square) in the image was magnified and is presented as an inset, showing clearly the lattice fringe of CdS nanocrystallite.

results in a locally disturbed  $\text{MoS}_2$  edge plane (white arrows) and  $\text{CdS}(\text{TP})_n$  rich domain (black arrows). Such guest extrusion is probably due to the mechanical strain along the  $(00l)$  direction upon thin-sectioning by ultramicrotome. A similar structural evolution has recently been reported by Marshall *et al.* for molecular cluster  $(\text{Co}_6\text{S}_8(\text{PPh}_3)_6)$  intercalated  $\text{MoS}_2$ , describing heterogeneities in the degree of pillaring of  $\text{MoS}_2$ .<sup>17</sup> As expected from such microscopic evolution, the selected area electron diffraction (SAED) pattern of the present nanohybrid composite only shows the diffused ring patterns, which are characteristic features of polycrystalline samples or disordered crystal systems (upper-left insert in Fig. 4). On the other hand, in contrast to the edge region of the cross-sectioned specimen, the micrograph from the inner region exhibits rather homogeneously distributed  $\text{CdS}(\text{TP})_n$  nanoparticles on the surface of disordered  $\text{MoS}_2$  sheets [Fig. 5]. The average size of  $\text{CdS}(\text{TP})_n$  was determined to be 6.5 nm. We could not observe any ordered stack of  $\text{MoS}_2$  sheets, reminiscent of the “house of cards” structure formed by two-dimensional  $\text{MoS}_2$  layers and zero-dimensional CdS quantum dots. This finding is highly consistent with the internal structure expected in FE-SEM analysis and our XRD results on this material.

It was expected from such structural characteristics that the removal of capping molecules (thiophenol) from the surface of CdS nanocrystallites by thermal degradation could afford the present material with nanoporosity that might have catalytic advantages due to the high surface area. Therefore, we have carried out nitrogen adsorption-desorption isotherm experiments at liquid nitrogen temperature (77 K) with a computer-controlled measurement system. The calculated Brunauer–Emmett–Teller (BET) specific surface areas ( $S_{\text{BET}}$ ) of the present nanohybrid ( $\text{CdS-MoS}_2$ ) are presented in Table 2 together with those of the pristine 2H- $\text{MoS}_2$  and exfoliated–restacked compound for comparison. According to our surface area analyses, the exfoliated–restacked  $\text{MoS}_2$  exhibits an order of magnitude higher BET specific surface area ( $15 \text{ m}^2 \text{ g}^{-1}$ ) compared to the pristine material (2H- $\text{MoS}_2$ ), whereas the present nanohybrid ( $\text{CdS-MoS}_2$ ) shows a value ( $\sim 84 \text{ m}^2 \text{ g}^{-1}$ ) nearly two orders of magnitude higher. Such an increased specific surface area of the nanohybrid sample again supports the microscopic evolution of the internal structure of the  $\text{CdS-MoS}_2$  nanohybrid, and suggests that the present nanohybrid material can be successfully applied as a high performance hydrodesulfurization (HDS) or visible light

**Table 2** BET specific surface area of the pristine 2H- $\text{MoS}_2$ , exfoliated–restacked  $\text{MoS}_2$ , and  $\text{CdS-MoS}_2$  nanohybrid.

	2H- $\text{MoS}_2$	exfoliated–restacked $\text{MoS}_2$	$\text{CdS-MoS}_2$ nanohybrid <sup>a</sup>
$S_{\text{BET}}/\text{m}^2 \text{ g}^{-1b}$	1	15	84

harvesting catalyst. Catalytic activity tests on this nanohybrid are currently in progress.

## Conclusion

In this work, we have demonstrated that the nanohybridization technique could be an effective method for developing new functional materials from known substances to generate a novel quantum dot pillared transition metal dichalcogenide ( $\text{CdS-MoS}_2$ ). According to our microscopic investigations on the present nanohybrid material, we have found that zero-dimensional semiconducting CdS nanocrystallites ( $\sim 6.5 \text{ nm}$ ) are successfully immobilized by two-dimensional  $\text{MoS}_2$  lamellae, forming a “house of cards” structure. Such structural characteristics lead to an increase in BET surface area by two orders of magnitude ( $\sim 84 \text{ m}^2 \text{ g}^{-1}$ ) compared to the pristine 2H- $\text{MoS}_2$ , suggesting that the present nanohybrid material can be successfully applied to the high performance catalyst in hydrodesulfurization (HDS) and/or visible light harvesting system. We are very confident that our nanohybridization approach for synthesizing new functional materials can be successfully extended to other materials.

## Acknowledgement

The work was supported partly by the Korean Science and Engineering Foundation through the Center for Molecular Catalysis and by the Korean Ministry of Science of Technology through the National Research Laboratory Project. W. Lee and T.-J. Yoon are grateful for the award of a BK21 fellowship.

## References

- 1 J. H. Choy, Y. I. Kim and S. J. Hwang, *J. Phys. Chem. B*, 1998, **102**, 9191.
- 2 J. H. Choy, S. J. Kwon and G. S. Park, *Science*, 1998, **280**, 1589.
- 3 J. H. Choy, S. Y. Kwak, Y. J. Jeong and J. S. Park, *Angew. Chem., Int. Ed.*, 2000, **39**, 4041.
- 4 W. M. R. Divigalpitiya, R. F. Frindt and S. R. Morrison, *Science*, 1989, **246**, 369.
- 5 L. Wang, J. Schindler, J. A. Thomas, C. R. Kannewurf and M. G. Kanatzidis, *Chem. Mater.*, 1995, **7**, 1753.
- 6 R. Bissessur, M. G. Kanatzidis, J. L. Schindler and C. R. Kannewurf, *J. Chem. Soc., Chem. Commun.*, 1993, 1582.
- 7 R. Bissessur, J. Heising, W. Hirpo and M. Kanatzidis, *Chem. Mater.*, 1996, **8**, 318.
- 8 F. Wypych and R. Schollhorn, *J. Chem. Soc., Chem. Commun.*, 1992, 1386.
- 9 J. Heising and M. G. Kanatzidis, *J. Am. Chem. Soc.*, 1999, **121**, 11720.
- 10 K. E. Dungey, M. D. Curtis and J. E. Penner-Hahn, *J. Catal.*, 1998, **175**, 129.
- 11 In unilamellar  $\text{MoS}_2$  each molybdenum atom is octahedrally coordinated with six sulfur atoms and each octahedron extends two-dimensionally, sharing its edges to form a single sheet. In other words, the molybdenum atoms are positioned at the center of two hexagonal sulfur planes, forming a metal plane. Although the difference in electron densities of Mo (atomic number 42) and

S (atomic number 16) is rather large, it could not give significant image contrast due to lack of resolution of the TEM that was employed in the present microscopic investigations.

- 12 J. Heising and M. G. Kanatzidis, *J. Am. Chem. Soc.*, 1999, **121**, 638.
- 13 J. Heising, F. Bonhomme and M. G. Kanatzidis, *J. Solid State Chem.*, 1998, **139**, 22.
- 14 A. N. Goldstein, C. M. Echer and A. P. Alivisatos, *Science*, 1992, **256**, 1425.
- 15 J. P. Wilcoxon, R. L. Williamson and R. Baughman, *J. Chem. Phys.*, 1993, **98**, 9933.
- 16 We have attempted to determine the atomic ratio of Mo : Cd : S in the present nanohybrid by EDAX elemental analyses by probing various regions of the sample under morphology investigations. The presence of Cd in our nanohybrid sample was certified by EDAX analyses. However, it turned out that EDAX elemental analyses could not provide any convincing quantitative information, yielding only qualitative results since the *K* X-ray edge of sulfur overlaps significantly with the *L<sub>a</sub>* edge of molybdenum, resulting in underestimation of the molybdenum content.
- 17 J. Brenner, C. L. Marshall, L. Ellis and N. Tomczyk, *Chem. Mater.*, 1998, **10**, 1244.